Using raindrops to constrain past atmospheric density

Lucas Kavanagh[a,b,*], Colin Goldblatt[a]

[a] *University of Victoria, Bob Wright Centre, 3800 Finnerty Road, Victoria British Columbia, Canada V8P 5C2*
[b] *McGill University, Adams Building, 3450 University Street, Montreal Quebec, Canada H3A OE8*

Abstract

There exists a dearth of constraints on the physical properties of the early Earth atmosphere. The Som palaeopycnometry method estimates an upper limit on ancient atmospheric density based on the size of lithified raindrop imprints preserved in ancient strata, with the assumption that the largest imprint was made by the largest possible raindrop. Using this technique *Som et al.* (2012) proposed a constraint on Archean atmospheric density of less than $2.3\,\mathrm{kg\,m^{-3}}$. Applying this method to modern raindrop imprints, the upper bound on surface density produced is $0.9\,\mathrm{kg\,m^{-3}}$, lower than the actual value of $1.2\,\mathrm{kg\ m^{-3}}$, refuting the method. We propose several changes to the method, the most important of which is increasing the maximum possible drop size from 6.8 to 10 mm to be consistent with new large datasets of raindrop observations. With these changes, our upper bound on modern surface density becomes $2.7\,\mathrm{kg\,m^{-3}}$, a valid limit. The upper bound on Archean atmospheric density is then revised to $11.1\,\mathrm{kg\,m^{-3}}$. In general, we find that raindrop imprint size distribution depends much more strongly on rainfall rate than atmospheric density, which translates into large errors. At best, the precision of raindrop palaeopycnometry will be a factor of a few to an order of magnitude.

Keywords: Palaeobarometry, Raindrops, Archean, Pressure, Density, Faint Young Sun

*Principal corresponding author, phone number: +1 514-834-4003
Email addresses: lucas.kavanagh@mcgill.ca (Lucas Kavanagh), czg@uvic.ca (Colin Goldblatt)

1. Introduction

The mass of the Archean atmosphere, and hence surface pressure, has generally been regarded as unconstrained. The bulk atmospheric composition of Earth today is 78% di-nitrogen, 21% di-oxygen and 1% argon. Previous constraints on Archean atmospheric composition are geochemically based, relating to individual constituents. Oxygen is best constrained; it was only a trace gas during the Archean (e.g. *Holland*, 1984; *Farquhar et al.*, 2000). Nitrogen may have been up to three times present level, given the size of the bulk silicate Earth nitrogen inventory (*Goldblatt et al.*, 2009). Palaeosol constraints indicate that carbon dioxide was a minor species though the Proterozoic (*Sheldon*, 2006), but this is presently unconstrained during the Archean; very high levels (tens of bars) are possible in theory, given the size of the oxidised geologic carbon inventory.

Historically, a qualitative physical constraint on the density of atmosphere was proposed by *Lyell* (1851). He noted that the size distribution of lithified Phanerozoic raindrop imprints was qualitatively similar to modern imprints, implying a similar atmospheric density. Given that carbon dioxide is constrained to be a minor species during the Phanerozoic (e.g. *Royer*, 2006), the mean molecular weight of the atmosphere would be similar to today and pressure would thus have been similar.

Recently, *Som et al.* (2012) proposed a quantitative method to use such raindrop imprints as a palaeopycnometer (measure of past density) and applied this to Neoarchean fossil imprints thought to have formed at sea level. Their method relies solely on the largest preserved raindrop imprint, taken to be caused by some theoretical maximum raindrop size, yielding a hard upper bound on density, or a "likely" largest raindrop, yielding a "likely" upper bound on density. This method uses an empirical transfer function to relate imprint crater diameter to drop momentum and, with an assumed drop size, recovered terminal velocity and hence atmospheric density. Proposed values are a hard upper bound of

$2.3\,\mathrm{kg\,m^{-3}}$ or a "likely" upper bound of $1.3\,\mathrm{kg\,m^{-3}}$, compared to modern mean surface density of $1.2\,\mathrm{kg\,m^{-3}}$. For given atmospheric mass (surface pressure), density depends on temperature and mean molecular weight; assuming modern mean surface temperature and a di-nitrogen bulk composition gives hard and "likely" upper bounds on pressure of 2000 hPa and 1100 hPa, whereas modern sea-level pressure is 1000 hPa. Likely temperature variation gives a 10% uncertainty. A carbon dioxide bulk composition would reduce pressure by a third. The Som method has also been applied to samples of Permian age by *Glotzbach and Brandes* (2014) who proposed an upper bound on density during that period of $2.3\,\mathrm{kg\,m^3}$.

The purpose of this paper is to critically analyze the quantitative method introduced by *Som et al.* (2012) and give our resulting re-interpretation of the Archean data. The structure of the paper is as follows: in section 2, we describe the Som method, in section 3 we present our analysis of it and propose revisions, in section 4 we test the original and revised method with modern raindrop imprints, followed by discussion and conclusions.

2. An Outline of the Som Palaeobarometry Method

In order to present a coherent analysis, we begin by reviewing the Som method and the theoretical basis for it. The method (summarized in Figure 1) is split into two key procedures: an experimental calibration to relate crater area to the momentum of the drop responsible (Figure 1, orange path) and the procedure for calculating atmospheric density from the drop momentum inferred from preserved raindrop imprint (Figure 1, green path).

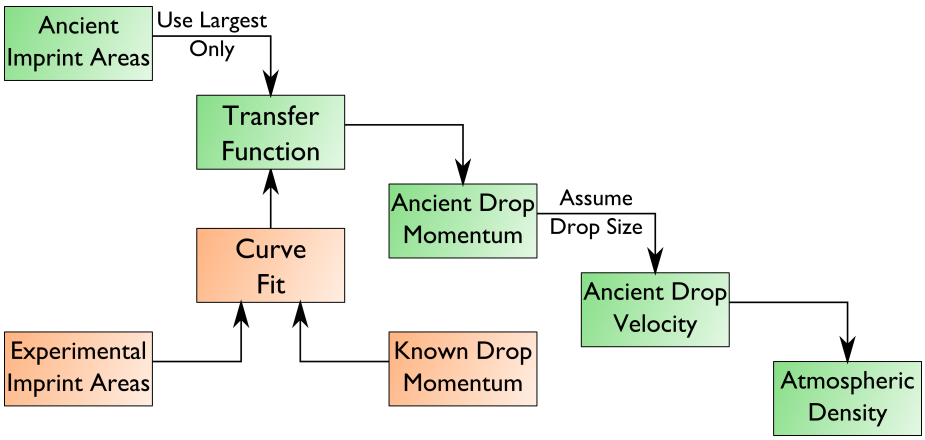

Figure 1: A flowchart outlining the basics of the Som method. The green boxes represent the path that data collected in the field takes, the orange boxes represent the calibration of the transfer function.

2.1. Theoretical Basis

The dominant forces of a falling raindrop are gravity acting downwards and air resistance (drag), acting upwards. When these are balanced, the raindrop has reached terminal velocity. Experimentally, the largest drops reach this after falling for 12 m; smaller drops will achieve this sooner (*Gunn and Kinzer*, 1949).

A common misconception is that raindrops are shaped like teardrops. High-speed photography by *Matthews and Mason* (1965) shows the lifecycle of raindrops (Figure 2). They begin spherical, but soon develop a flat bottom due to air resistance. Deformation continues, causing the drop to inflate and form a parachute of water, supported by a thick rim at its base. This inverted bag continues to grow until the external aerodynamic forces are greater than the surface tension and hydrostatic pressure of the drop. At this point the top breaks and the entire drop shatters into smaller droplets of varying size (*Villermaux and Bossa*, 2009). A fundamental consequence of this evolution of droplet shape is the existence of a maximum droplet size (*Clift et al.*, 1978), which is relied on heavily in the Som method. We will show later that size of this assumed maximum is of critical importance.

The life of a raindrop ends suddenly when it impacts the substrate below. If the substrate can be deformed easily, the impacting drop will form a crater. The formation of a crater depends upon the mass and velocity of the impacting drop and the properties of the sediment (shear strength, water content and compaction) (*Ghadiri*, 2004).

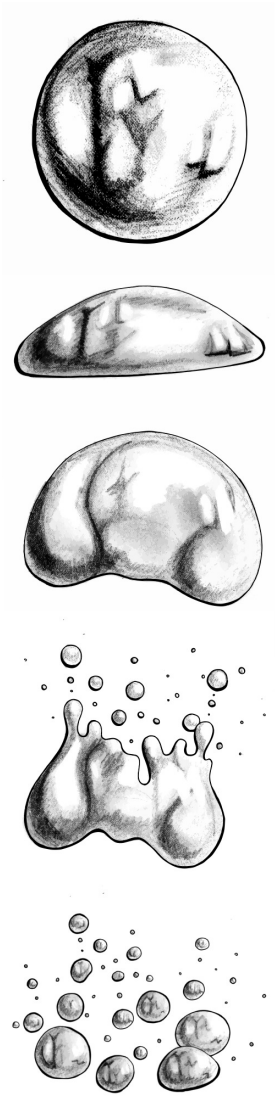

Figure 2: A series of sketches by Kelsey Hemphill showing the breakup process of raindrops, based on photographs by *Villermaux and Bossa* (2009).

2.2. Calibration

Som et al. (2012) defined a dimensionless momentum term (J) of falling drops,

$$J = \frac{V_t m_d}{\eta A_d} \tag{1}$$

in terms of the terminal velocity of the drop (V_t), its mass (m_d), its cross sectional area (A_d), and the dynamic viscosity of the atmosphere (η). Artificial raindrops were auto-pipetted from the top of a stairwell high enough for drops to reach terminal velocity before landing in a tray of sediment. The sediment that *Som et al.* (2012) used was moistened volcanic ash from the 2010 eruption of Eyjafjallajökull, chosen to replicate the substrate in which the Archean imprints are preserved. The artificially created imprints were coated with a combination of hair spray and urethane resin and their cross sectional areas were measured using a high resolution 3-D laser scanner. Dimensionless momentum was calculated for each volume trial with dynamic viscosity treated as a constant value of 1.78×10^{-5} Pa s (this has only a weak temperature dependence). To find the terminal velocity, the Reynolds number was calculated through the method of *Berry and Pranger* (1974), taking the drop diameter as the characteristic length scale, velocity was solved for:

$$V_t = \frac{Re\eta}{2r_d\rho_a} \tag{2}$$

Where ρ_a is the density of the atmosphere and r_d is the radius of the drop (assuming a spherical drop).

The mean imprint areas were plotted against the dimensionless momenta of the drops that created them. A quadratic calibration curve was then fitted in log space to allow for a conversion between drop momentum and crater area (Figure 3).

2.3. Archean Imprints

Som et al. (2012) examined raindrop imprints preserved in a 2.7 Ga sample of lithified volcanic ash, located on eighteen stratigraphic levels (Roger Buick, personal communication, August 5^{th}, 2013) of the Ventersdorp Supergroup in

South Africa (*Van der Westhuizen et al.*, 1989). Preservation is particularly good as thin layers of fine ash formed a protective covering over the craters after they formed in coarser ash.

Using the transfer function from stairwell calibration experiments, dimensionless momenta were retrieved from measures crater areas. Momentum is function of mass and velocity. With the assumption that drops are falling at terminal velocity, velocity is a function of droplet mass and atmospheric density. Thus to retrieve density, droplet mass must be assumed. *Som et al.* (2012) used only the largest measured crater, with the assumption that this was made by the largest raindrop.

Two calculations of atmospheric density were made: "absolute" and "likely" upper limits. For the absolute limit, *Som et al.* (2012) took the droplet size to be what they considered to be the largest drop ever recorded at ground level, 6.8 mm in diameter (*Willis and Tattelman*, 1989). The likely upper limit was taken as the upper extreme of a drop size distribution from a heavy rainfall event (the validity of both of these limits are evaluated below). Hence *Som et al.* (2012) gave an absolute limit on Archean density of $2.3\,\mathrm{kg\,m^{-3}}$ and a range of likely maxima from 0.6 to 1.3 $\mathrm{kg\,m^{-3}}$. Modern atmospheric density is $1.2\,\mathrm{kg\,m^{-3}}$.

3. Methodological Evaluation

We now proceed to evaluate the Som method. We first replicate the sediment calibration, then test a number of methodological assumptions against a large dataset of modern raindrops. Finally, we derive a model producing idealized crater area distributions, dependant on atmospheric density and rainfall rate to the test method's sensitivity to each.

3.1. Stairwell Calibration

We repeated the stairwell calibration experiments in a 19.2 m stairwell, using a fine quartz beach sand collected from Gonzales Beach in Victoria, B.C., sieved to less than 1 mm as substrate. We then photographed the trays of substrate,

and digitally measured the crater areas using ImageJ, a software package created by the National Institutes of Health (Figure 3). Figure 4 compares micrographs of Gonzales Beach sand with the Eyjafjallajökull ash used by *Som et al.* (2012); note the higher visible clay content in the ash. An advantage of the substrate that we use is a plentiful supply, so we were able to measure more imprints than *Som et al.* (2012) (392 versus 172), over a wider range of volumes (10.5 to 143.7 μL versus 10.5 to 79.8 μL) and with more drops per volume.

Formation of craters involves both the transport and compaction of the sediment beneath the projectile. Both these processes require work to displace sediment; as energy is defined as the ability to do work, we consider the appropriate quantity to use in a transfer function to be kinetic energy, rather than momentum as used by *Som et al.* (2012). Using kinetic energy in relation to crater sizes is standard in planetary geology, with theoretical relationships of $A \propto \mathrm{KE}^{\frac{1}{2}}$ for a projectile displacing sediment and $A \propto \mathrm{KE}^{\frac{2}{3}}$ for a projectile compacting sediment (*de Pater and Lissauer*, 2010). With near vertical rainfall onto poorly compacted sediment, compaction is the more likely process.

Examining Figure 3, we see a log-linear fit between kinetic energy and imprint area for both datasets. The exponents are similar to the theoretical prediction of 2/3, supporting compaction as the dominant process. We do not see sufficient evidence of curvature to introduce a quadratic term, as *Som et al.* (2012) did, and this is not supported by theory. A change in atmospheric density alters a drops kinetic energy through its terminal velocity. We alter kinetic energy by changing drop mass, as changing air density for the purpose of this experiment is challenging. Perhaps a future study could calibrate craters by performing this experiment at a wide range of elevations.

Good agreement between the theoretical prediction of a relationship between kinetic energy and crater area for compaction craters in two datasets supports the use of this as a transfer function. However, note the offset between curves: drops with the same kinetic energy made larger craters in sand, likely due to a higher clay fraction (cohesiveness) in the ash. It follows directly that correctly matching sediment properties is essential to proper calibration. As an example,

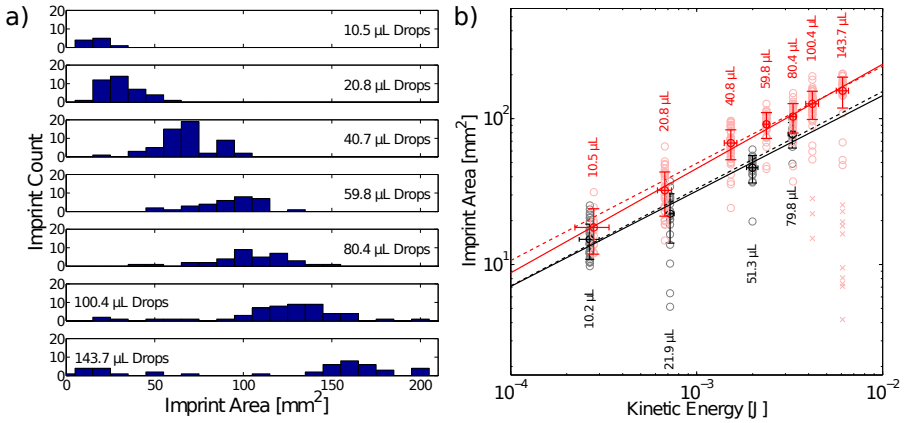

Figure 3: **a** Histograms of imprint area from our trials. Note generally increasing imprint size with drop volume, and evidence of raindrip breakup for the larger drops (seen as small imprints from fragmented drops). **b** Calibration of cross sections crater area to the kinetic energy of raindrops. The red data is from this study (solid line is the best fit of $A = KE^{0.71} + 8.7558$, $r^2 = 0.76$), the black is that of *Som et al.* (2012) ($A = KE^{0.65} + 7.9802$, $r^2 = 0.87$) and the dashed lines are forced to the theoretical exponent of 2/3: $A = KE^{2/3} + 8.5$ (for our data) and $A = KE^{2/3} + 8.1$ (for that of *Som et al.* (2012)). Error bars represent one standard deviation.

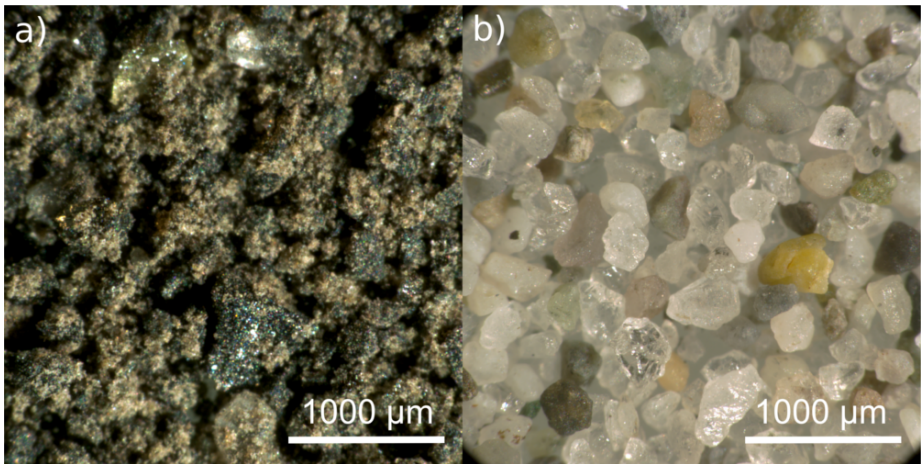

Figure 4: Micrographs of a) the volcanic ash used by *Som et al.* (2012) and b) the quartz beach sand used in this study.

applying our calibration curve rather than Som's to the Archean increases the proposed upper limit on density increased by a factor of two.

3.2. Modern Rainfall Characteristics

The assumed size of the largest raindrop and the frequency of large drops in a given sample size are critical to the Som method. To evaluate these, we use a dataset of over 13 million raindrops measured by optical disdrometers as part of the NASA Midlatitude Continental Convective Clouds Experiment (MC3E) near Lamont Oklahoma from April to June 2011 (optical disdrometers measure the size and speed of raindrops falling through a laser beam, based on the amplitude and length of the drop in the beam signal (*Loffler-Mang and Joss*, 2000)). The data are shown in Figure 5.

Som et al. (2012) used a 6.8 mm drop, observed by *Willis and Tattelman* (1989) as their largest size. Examining Figure 5, it is plainly visible that larger drop sizes exist, with numerous drops in the 9-10 mm bin. This is consistent with the theoretical prediction by *Clift et al.* (1978) of a 10 mm maximum. Using 10 mm as the maximum drop size increases the absolute upper limit on Archean density by a factor of two.

Figure 5 displays a pattern of drop frequency decreasing exponentially with drop size. Normalizing each day of rainfall produces the lower plot in Figure 5 which suggests the inverse sample size required to expect to see a particular size of drop. The inverse sample size of *Som et al.* (2012) (955^{-1}) is plotted as a solid black horizontal line, suggesting that they would have likely observed a largest drop of 3 to 9 mm, depending on rainfall rate. To observe 10 mm drops, one would likely need a sample size of at least of 3000 (the dotted black line in Figure 5) for the heaviest rain, or $\sim 10^6$ for light rain.

To define their 'likely" maximum, *Som et al.* (2012) took the largest 0.2% of drops in a 100 mm hr^{-1} rainfall event (implying a sample size of 500) from four drop size distributions (*Willis and Tattelman* (1989), *Marshall and Palmer* (1948), *Ochou et al.* (2007)), giving a range of likely maxima of 3.8-5.3 mm. A high rainfall rate was chosen to maintain the upper limit (by assumption, the

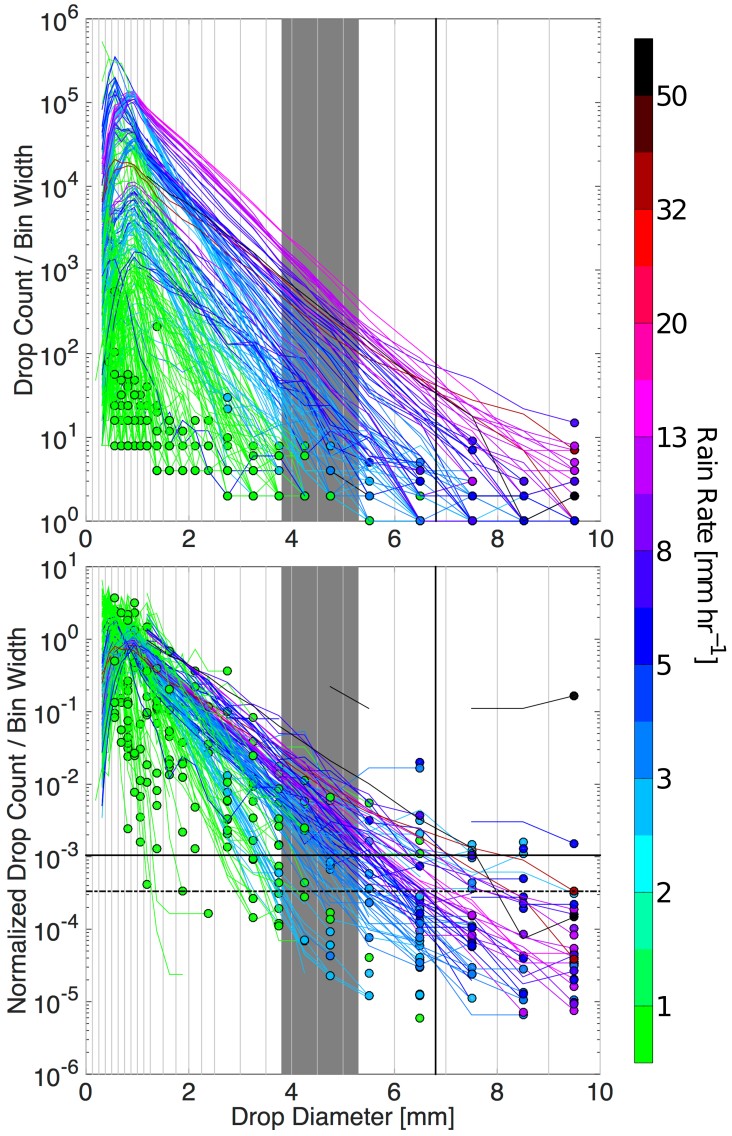

Figure 5: Disdrometer data from MC3E. The bottom plot has been normalized so the area under each curve is 1. Each line is a day with recorded rainfall, coloured according to rainfall rate. Each point in the maximum drop size observed on that day. The solid horizontal line corresponds to the sample size of *Som et al.* (2012) and the dashed horizontal line is the inferred minimum size to likely sample the largest possible drops. The shaded grey area is the "likely" upper limit (3.8-5.8 mm) and the vertical black line is the "absolute" upper limit (6.8 mm) assumed by *Som et al.* (2012).

ancient rainfall rate was likely much less). The validity of these maxima can be tested directly against this modern dataset. The observed maximum daily drop size fell below Som's "likely" maximum range (<3.8 mm) in 46.0% of events, within Som's "likely" maximum range (3.8-5.8 mm) in 17.8% of events, between Som's "likely" and "absolute" maxima (5.8-6.8 mm) in 12.0% of events, and above Som's "absolute" maximum in (>6.8 mm) 24.3% of events. Thus, the Som definition of a "likely" upper limit on Archean density is refuted.

To check that this result is not dependant on the type of disdrometer used, we examined the data from a 2-dimensional video disdrometer placed at the same site, which observed drops up to 9.0 mm in diameter and found the maximum drop size to be above >6.8 mm on 14.1% of the days with rainfall sampled.

3.3. A Model of Raindrop Cratering

Raindrop imprint area is a function of both drop size (larger drops give bigger imprints) and atmospheric density (higher density slows drops, giving smaller imprints). Figure 6 was created by calculating the terminal velocity of drops ranging in size from 3 to 10 mm, in atmospheres ranging from 0 to 5 $kg\,m^{-3}$. The craters resulting from these virtual drops were found using our empirical transfer function. With known density in the modern atmosphere, we observed maximum imprint sizes ranging in area from 23 to 222 mm^2, by inference caused by drops between 3 and 7.5 mm diameter. By extension, constraining drop size is critical for palaeopycnometry.

A well known feature of rainfall events is that larger drops are more likely with higher rainfall rates (*Marshall and Palmer*, 1948); this can be seen in Figure 5 and is shown explicitly in Figure 7. This begs the question: what is the dominant influence on crater size distributions, atmospheric density or rainfall rate? To evaluate this, we create a model that generates a raindrop size distribution based on a 3 parameter gamma function (*Tokay and Short*, 1996):

$$N(D) = N_0 D^{\mu} exp(-\Lambda D) \tag{3}$$

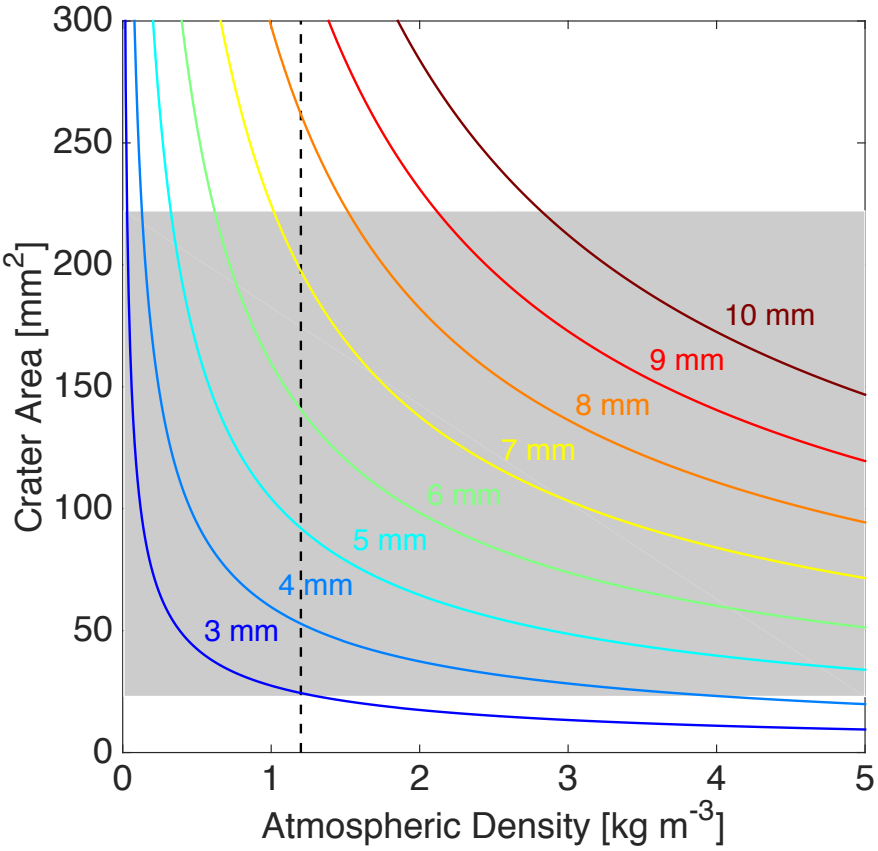

Figure 6: The sensitivity of crater areas to atmospheric density at varying drop sizes. The shaded grey are is the range of maximum imprint areas observed in modern rainfall events and the dashed line is modern atmospheric density.

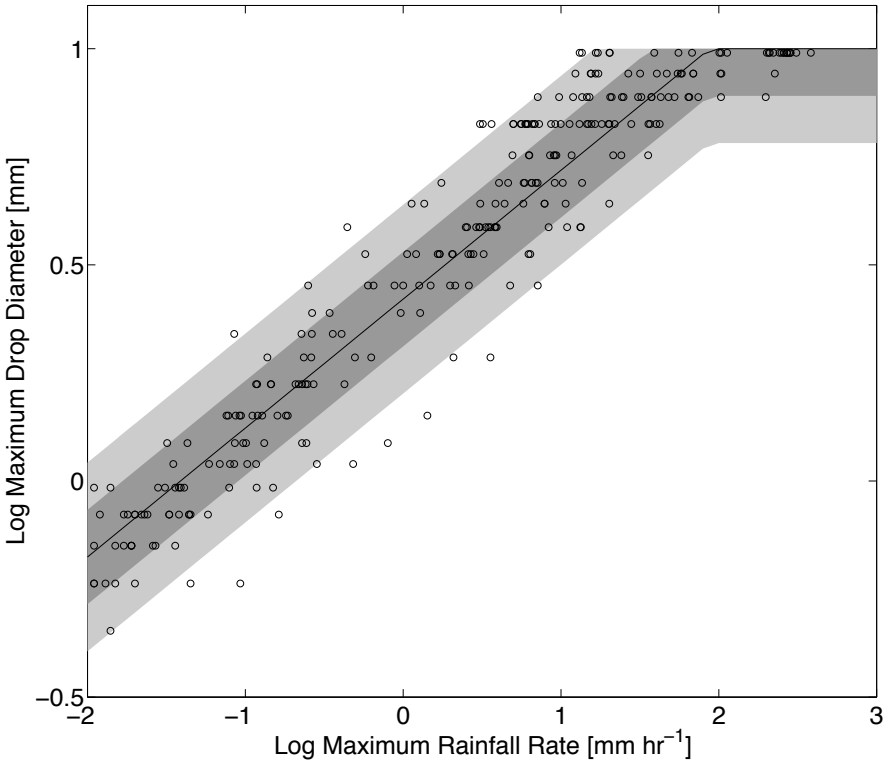

Figure 7: Maximum drop diameter from rainfall events in MC3E data (black circles) as a function of maximum rainfall rate. The black line is the best fit, dark and light grey areas are one and two standard deviations around the mean respectively.

Where $N(D)$ is the number of drops per diameter D per cubic meter of air, N_0 is the intercept parameter, μ is the shape parameter and Λ is the slope parameter. We used the value of $8 \times 10^4\ mm^{-1}m^{-3}$ for N_0 and the rate dependent slope parameter of $\Lambda = 4.1R^{-0.21}\ mm^{-1}$ (*Marshall and Palmer*, 1948). The exponent of this relationship as well as the shape parameter (μ) were tuned to fit an approximate upper limit on the data in Figure 7, producing values of -0.34 and 8 respectively. A maximum drop diameter of 10 mm was also imposed on this model.

We then simulate imprint areas for a range of rainfall rates and atmospheric

densities. For a given rainfall rate, a drop size distribution is calculated with Equation 3.3. For given density, terminal velocity is calculated for each drop following *Lorenz* (1993). We began with an initial guess of terminal velocity though the method of (*Berry and Pranger*, 1974), which is then iteratively modified to account for changes in the drag coefficient resulting from drop deformation. This is an important change as drop deformation is particularly relevant at large drop sizes (*Lorenz*, 1993). The velocity is given by:

$$V_t = \sqrt{\frac{2mg}{\rho_a S C_d}} \tag{4}$$

Where S is the surface area of the drop, g is acceleration due to gravity, and C_d is the drag coefficient given by:

$$C_d = \frac{24}{Re}(1 + 0.197Re^{0.63} + 2.6 \times 10^{-4} Re^{1.38}) \tag{5}$$

These are modified by the flattening ratio of the drop, k (which is linearly related to the webber number):

$$S = S_o k^{-\frac{2}{3}} \tag{6}$$

$$C_d = \frac{C_d}{k} \tag{7}$$

This processes is iterated until the modified drag and surface areas produce a negligible change in terminal velocity. Once drop velocity is known, kinetic energy may be found and imprint area calculated via the transfer function. Simulated crater size distributions are shown in Figure 8 for reasonable ranges of rainfall rate (0.25, 2.5 and 25 mm hr^{-1}) and atmospheric density ($\frac{1}{3}$, 1, 3, and 10 times modern density). The degeneracy between rainfall rate and density is immediately apparent: high rainfall rate at low density will produce a similar distribution as a low rainfall rate at high density.

Further, it is apparent that rainfall rate is capable of exerting a stronger control over imprint area distribution than air density. Figure 8 shows idealized crater distributions over a wide range of air densities possible on a billion-year timescale (0.3 to 10 $\mathrm{kg\,m}^{-3}$) and modern rainfall rates (0.25 to 25 $\mathrm{mm\,hr}^{-1}$). Consider, for example a change in rainfall rate from 0.25 to 25 $\mathrm{mm\,hr}^{-1}$ and

assume a sample size of 1000 imprints and modern atmospheric density. The largest observed crater would increase from 8 to 242 mm^2, a factor of 30. However, if we hold rainfall rate constant at 2.5 $\mathrm{mm\,hr}^{-1}$ and decrease atmospheric density from three times to a third modern density, roughly the range considered possible by *Som et al.* (2012), we increase the crater size from 25 to 109 mm^2 a factor of 4. It is problematic that a reasonable variation of rainfall rate can exert considerably more control than a drastic change in atmospheric density. Whilst there is considerable uncertainty and variation in drop size distributions and our model is not a unique solution, we take comfort in that every parameterization we tried gave the same qualitative result of rainfall rate easily being a primary control on crater distributions.

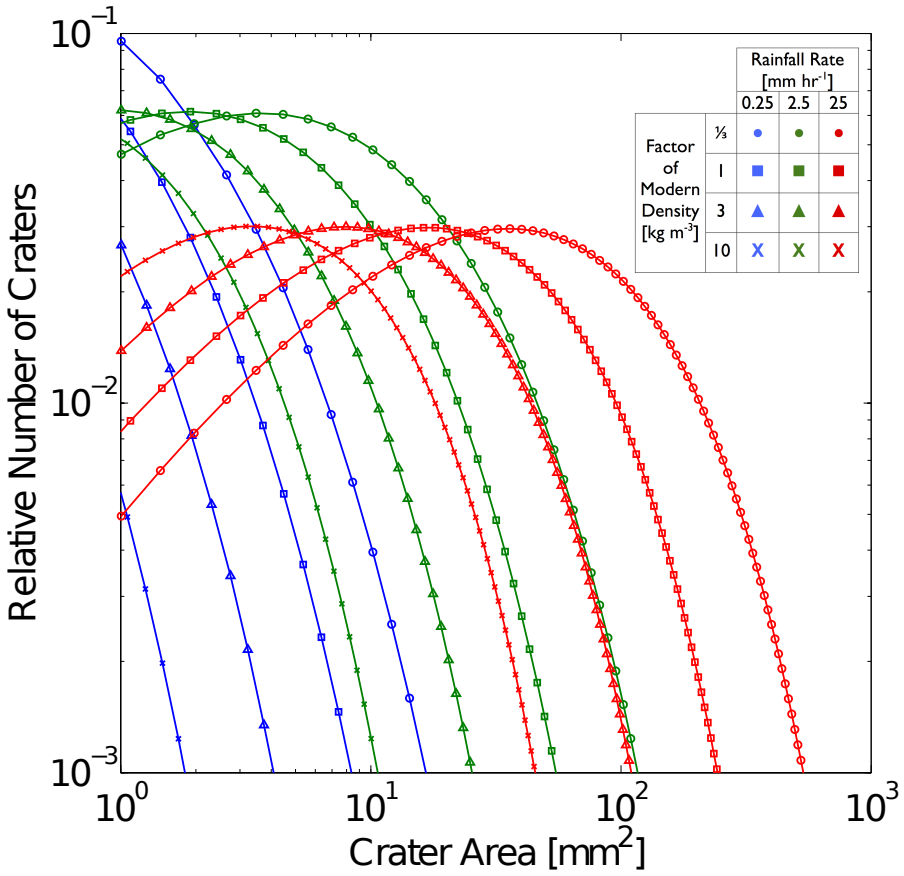

Figure 8: Modelled distributions of crater areas, dependent on rainfall rate and atmospheric density.

4. Modern Verification

We measured raindrop imprints shortly after formation from 6 modern rainfall events on Gonzales Beach, from which our calibration sediment was taken, and one event from each of Cadboro Bay (Victoria, BC), and Milties Beach (Vargas Island, BC) to take advantage of higher rainfall rates (both these beaches have similar sand to Gonzales). The Som method uses the single largest crater from all sampled events (recall that they sampled 18 stratigraphic levels). Treating our dataset in the same way (Table 1), we get an "absolute maximum" modern density of 0.9 $\mathrm{kg\,m^{-3}}$. Given modern atmospheric density of $1.2\,\mathrm{kg\,m^{-3}}$, this refutes the Som method.

We propose several modifications to the method: a transfer function in terms of kinetic energy instead of dimensionless momentum, drop terminal velocity is calculated using the method of *Lorenz* (1993) instead of *Berry and Pranger* (1974) and the absolute limit on atmospheric density is found by assuming a drop size of 10 mm in diameter instead of 6.8 mm (Table 1). With the ensemble of our modern rainfall events, this produces an absolute maximum density of $2.7\,\mathrm{kg\,m^{-3}}$, consistent with the known value. Each individual event is consistent too.

An advantage of our field sites on Vancouver Island is a dense network of weather stations from the Vancouver Island School Based Weather Network (*Weaver and Wiebe*, 2006). Stations, equipped with tipping bucket rain gauges, are located 600 m from Gonzales Bay, 80 m from Cadboro Bay and 8.2 km from Miltes Beach. Maximum drop size was estimated from the fit in Figure 7, with error propagated from there. All but one of our modern events gives a density which is correct within error. Although an interesting demonstration, this is sadly of little practical use there is no local record of Archean rainfall rate that we are aware of.

The record from Gonzales beach on 22/02/2013 includes a large maximum imprint area with a low rainfall rate, so gives a very low and evidently erroneous density estimate. This has to be taken as instructive, with several options. First

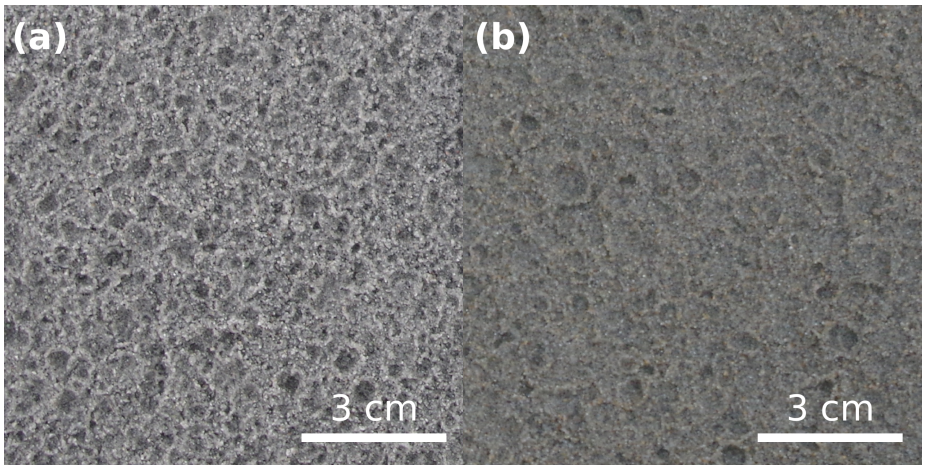

Figure 9: Examples of modern imprints preserved in sand at a) Gonzalies Beach and b) Milties Beach.

could be that there happened to be an unusually large raindrop, which would cast doubt on any limit other than the absolute maximum. Second, an ordinarily large maximum drop might have created an unusually large crater, perhaps due to the morphology of the sediment impacted (such as a patch of particularly unconsolidated sand). We did not propagate error from the transfer function between kinetic energy and imprint area and arguably should have done; this would increase the error bars on all results.

Table 1: Limits on modern and ancient atmospheric density, calculated using both the method of *Som et al.* (2012) and the modifications outlined in this study. Rate dependent limits were found using drop sizes produced using the upper-limit of the relationship in Figure 7. The event on 2013/02/21 does not have a rainfall rate as it only caused one tip of the tipping-bucket rain gauge. Values in bold are not consistent with known modern density.

Date	Location	Maximum Imprint Area [mm^2]	Rainfall Rate [mm hr^{-1}]	Som Method "Absolute" Limit [kg m^{-3}]	Som Method "Likely" Limit [kg m^{-3}]	This Study "Absolute" Limit [kg m^{-3}]	Rate Dependent Density (ρ^*) [kg m^{-3}]	$\rho^* - 2\sigma$, $\rho^* + 2\sigma$ [kg m^{-3}]
2013/01/08	Gonzales	44.6	1.93	4.8	2.9	24.7	0.7	0.1, 4.3
2013/02/21	Gonzales	23.0	-	9.5	5.6	60.6	-	-
2013/02/22	Gonzales	39.8	0.99	5.5	3.2	28.9	0.3	0.02, 2.5
2013/02/22	Gonzales	68.3	0.44	3.1	1.8	13.8	**0.05**	**-, 0.4**
2013/03/12	Gonzales	81.2	2.05	2.6	1.5	10.9	0.3	0.03, 2.0
2013/09/05	Gonzales	55.7	3.97	3.9	2.3	18.2	1.2	0.1, 6.4
2013/09/28	Milties	222.1	11.98	**0.9**	0.5	2.7	0.5	0.1, 2.5
2014/03/10	Cadboro Bay	70.8	4.36	3.1	1.8	13.1	1.0	0.1, 5.0
Archean	Ventersdorp	50.0	-	2.3	1.3	11.1	-	-

5. Reinterpretation of the Archean Imprints

With our modifications to the Som method verified against modern data, we have some confidence in applying it to the Som dataset of 2.7 Ga imprints from the Ventersdorp. Using a transfer function of $A = \mathrm{KE}^{0.71} + 8.7558$, fit to Som's ash calibration, and a drop size of 10 mm, their largest crater of 50 mm^2 suggests an upper limit on Archean density of $11.1\,\mathrm{kg\,m^{-3}}$, and order of magnitude higher than present.

If rainfall rate was known—which of course it is not—we could estimate the actual density (Figure 10). One could make the assumption that a very high rainfall rate was not responsible. Justification for this could be an *a priori* assumption that high rates are rare, or that prolonged heavy rainfall might not preserve distinct craters. If the maximum rain rate was 20 mm/hr, the density would have been 4 +7.2/-2.8 $\mathrm{kg\,m^{-3}}$ (2σ). A lower rate would give a lower density. *Som et al.* (2012) make no assumptions about a maximum possible rainfall rate that would allow for preservation in volcanic ash and our observation of preservation at $12\,mm\,hr^{-1}$ can only be applied to the quartz sand at Miltes beach. However, due to the increased clay content observed in Figure 4, we can assume that the volcanic ash used by *Som et al.* (2012) would be capable of preserving craters from rainfall of at least this intensity. A possible line of future investigation would be to collect imprints from intense rainfall events using a variety of sediment types to provide a rough constant on rain rate. Alternatively, we may ask: was density higher or lower in the Archean? Neglecting error, a rainfall rate lower than 7 mm would imply lower density. Accounting for error at 1σ or 2σ, the threshold would be 3 or 0.2 mm. High error (low precision) is a problem throughout. Thus our preferred interpretation here is that Archean density was likely within a factor of a few of present.

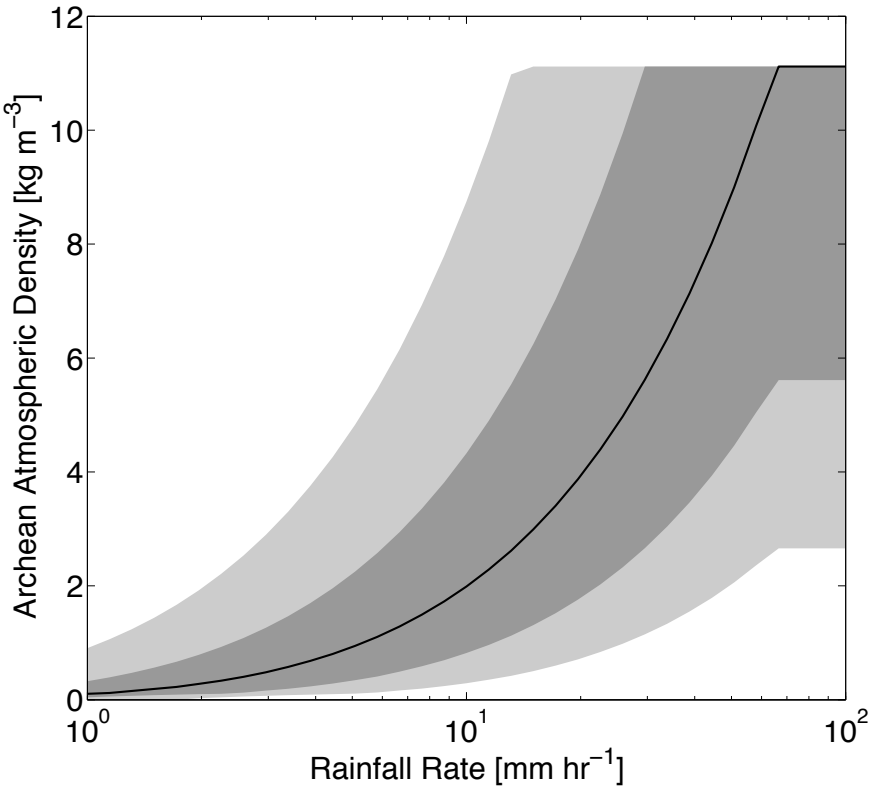

Figure 10: An estimate of Archean atmospheric density dependent on the maximum rainfall rate recorded in the Ventersdrop imprints. The shaded grey areas correspond to the upper and lower limits of drop size from Figure 7.

6. Conclusions

Som et al. (2012) proposed an algorithm to quantitatively estimate upper limits on past atmospheric density from lithified raindrop imprints, extending a qualitative proposal by *Lyell* (1851). In this paper, we have examined the theoretical and empirical support for these. For calculation of an absolute upper bound on density, we find support for the method in principle, but that the Som algorithm is invalidated by tests with modern imprints: an "absolute maximum" modern atmospheric density of $0.9\,\mathrm{kg\,m^{-3}}$ is found, which is less than the actual modern value of $1.2\,\mathrm{kg\,m^{-3}}$.

Hence we propose modifications to the algorithm: (1) assuming a maximum raindrop size of 10 mm, which has theoretical and empirical support (2) Using the method of *Lorenz* (1993) throughout to calculate drop terminal velocity, as this can model all relevant drop sizes self-consistently (3) Formulating the transfer function from drop mass and velocity to crater area in terms of kinetic energy rather than momentum, as there is theoretical support for this. With these modifications, we retrieve an upper limit on modern density of $2.7\,\mathrm{kg\,m^{-3}}$ and place an absolute upper limit on Archean density of $11.1\,\mathrm{kg\,m^{-3}}$.

Som et al. (2012) include an estimate of a "likely" upper limit on Archean density, based on estimates of the likely largest drop sizes. Comparison to modern disdrometer data show these assumptions to be invalid, leading us to reject these "likely" limits.

Crater size distribution is a function of both rainfall rate and atmospheric density, with rainfall rate likely exerting the primary control. In this sense, preserved raindrop imprints can best be seen as a palaeodistrometer. It would be more suitable to extend this to a palaeo-rain gauge than a palaeopycnometer. Use as a palaeobarometer, with embedded assumptions about atmospheric composition, is less suitable still.

The Som method treats this degeneracy by relying on the largest single imprint, and assuming that this comes from the largest raindrop. Clearly, relying on a single data point at the tail of a distribution (the maximum crater area)

does not lend itself to a high fidelity result. We see this in our modern data: low rainfall rates lead to inflated (but valid) values of "absolute maximum" density, as the largest actual raindrop will be smaller than the theoretical maximum. For a sample of imprints to include on or more which were actually caused by a raindrop at the theoretical maximum size would require both a high rainfall rate and an exceedingly large sample size.

For our modern cases, with known rainfall rates, we were able to successfully estimate modern density to within error, though note that this error is a factor of a few. By extension, if we make apparently reasonable assumptions about the rain rate responsible for the Archean imprints, we can infer that 2.7 Ga atmospheric density was within a factor of a few of present, with 2σ error of another factor of a few.

Thus, our conclusion is that lithified raindrop imprints do constrain Archean atmospheric density, though not to values as low as proposed by *Som et al.* (2012). The errors inherent in the method are between a factor of a few and an order of magnitude. High precision is not achievable with this method.

7. Acknowledgements

The authors would like to thank Sanjoy Som, David Catling, and Roger Buick for their discussion regarding their work as well as Kevin Zahnle for his general consultation and advice. The parsivel disdrometer data was obtained from the NASA Global Hydrology Resource Center (GHRC) DAAC, Huntsville, AL. http://ghrc.nsstc.nasa.gov/. Financial support was provided by a University of Victoria Jamie Cassels Undergraduate Research Award to L.K. and by a NSERC Discovery Grant and University of Victoria Professional Development funds to C.G.

References

Berry, E. X., and M. R. Pranger (1974), Equations for Calculating the Terminal Velocity of Water Drops, *Journal of Applied Meteorology*, *13*(1), 108–113, doi:

10.1175/1520-0450(1974)013.

Clift, R., J. Grace, and M. Webber (1978), *Bubbles, Drops and Particles*, 169–199 pp., Acedemic Press Inc., London.

de Pater, I., and J. J. Lissauer (2010), *Planetary Science*, 2nd ed., 177–184 pp., Cambridge University Press, Cambridge, New York.

Farquhar, J., H. Bao, and M. Thiemens (2000), Atmospheric influence of earth's earliest sulfur cycle, *Science*, *289*(5480), 756–758, doi:10.1126/science.289.5480.756.

Ghadiri, H. (2004), Crater Formation in Soils by Raindrop Impact, *Earth Surface Processes and Landforms*, *29*(1), 77–89, doi:10.1002/esp.1014.

Glotzbach, C., and C. Brandes (2014), Air density of the permian atmosphere: Constraints from lithified raindrop imprints, *Palaeogeography, Palaeoclimatology, Palaeoecology*, *409*(0), 280 – 289, doi:doi.org/10.1016/j.palaeo.2014.05.024.

Goldblatt, C., M. W. Claire, T. M. Lenton, A. J. Matthews, A. J. Watson, and K. J. Zahnle (2009), Nitrogen-Enhanced Greenhouse Warming on Early Earth, *Nature Geoscience*, *2*(12), 891–896, doi:10.1038/ngeo692.

Gunn, R., and G. D. Kinzer (1949), The Terminal Velocity of Fall for Water Droplets in Stagnant Air, *Journal of Meteorology*, *6*(4), 243–248, doi:10.1175/1520-0469(1949)006.

Holland, H. D. (1984), *The Chemical Evolution of the Atmosphere and Oceans*, 582 pp., Princeton University Press, Princeton.

Loffler-Mang, M., and J. Joss (2000), An optical disdrometer for measuring size and velocity of hydrometeors., *Journal of Atmospheric and Oceanic Technology*, *17*(2), 130, doi:10.1175/1520-0426(2000)017.

Lorenz, R. (1993), The life, death and afterlife of a raindrop on Titan, *Planetary and space science*, *31*(9), 647–655, doi:10.1016/0032-0633(93)90048-7.

Lyell, C. (1851), On Fossil Rain-marks of the Recent, Triassic, and Carboniferous Periods, *Quarterly Journal of the Geological Society*, *7*(1-2), 238–247, doi:10.1144/GSL.JGS.1851.007.01-02.40.

Marshall, J., and W. Palmer (1948), The Distribution of Raindrops with Size, *Journal of meteorology*, *5*(4), 165–166, doi:10.1175/1520-0469(1948)005.

Matthews, J. B., and B. J. Mason (1965), Electrification Produced by the Rupture of Large Water Drops in an Electric Field, *Quarterly Journal of the Royal Meteorological Society*, *91*(389), 379C380, doi:10.1002/qj.49709138919.

Ochou, A. B., N. a, and S. H (2007), Parameterization of Drop Size Distribution with Rain Rate, *Atmospheric Research*, *84*(1), 58–66, doi:10.1016/j.atmosres.2006.05.003.

Royer, D. L. (2006), Co2-forced climate thresholds during the phanerozoic, *Geochimica et Cosmochimica Acta*, *70*(23), 5665 – 5675, doi:dx.doi.org/10.1016/j.gca.2005.11.031.

Sheldon, N. D. (2006), Precambrian paleosols and atmospheric {CO2} levels, *Precambrian Research*, *147*(1 - 2), 148 – 155, doi:dx.doi.org/10.1016/j.precamres.2006.02.004.

Som, S. M., D. C. Catling, J. P. Harnmeijer, P. M. Polivka, and R. Buick (2012), Air Density 2.7 Billion Years Ago Limited to Less Than Twice Modern Levels by Fossil Raindrop Imprints, *Nature*, *484*(7394), 359–362, doi:10.1038/nature10890.

Tokay, A., and D. Short (1996), Evidence from tropical raindrop spectra of the origin of rain from stratiform versus convective clouds, *Journal of applied meteorology*, *35*, 355–371, doi:10.1175/1520-0450(1999)038.

Van der Westhuizen, W. A., N. J. Grobler, J. C. Loock, and E. A. W. Tordiffe (1989), Raindrop Imprints in the Late Archaean-Early Proterozoic Ventersdorp Supergroup, South Africa, *Sedimentary Geology*, *61*(3-4), 303–309, doi:10.1016/0037-0738(89)90064-X.

Villermaux, E., and B. Bossa (2009), Single-Drop Fragmentation Determines Size Distribution of Raindrops, *Nature Physics*, *5*(9), 697–702, doi:10.1038/nphys1340.

Weaver, A. J., and E. C. Wiebe (2006), Micro Meteorological Network in Greater Victoria Schools, *CMOS Bulletin*, *34*(6), 184–190.

Willis, P., and P. Tattelman (1989), Drop-Size Distributions Associated with Intense Rainfall, *Journal of Applied Meteorology*, *28*(1), 3–15, doi:10.1175/1520-0450(1989).